INFLUENCE OF THE TRACTION-SEPARATION COHESIVE LAW ON THE ADHESIVELY-BONDED REPAIR FAILURE LOAD

Lorena M. Fernández-Cañadas*, Elena M. Moya-Sanz*, Inés Iváñez* and Sonia Sánchez-Sáez*

*Department of Continuum Mechanics and Structural Analysis
University Carlos III of Madrid
Avda. de la Universidad 30, 28911 Leganés, Madrid, Spain

e-mail: lormoren@ing.uc3m.es, web page: http://www.uc3m.es/mma

Keywords: composite repairs, thin laminates, cohesive zone model.

Abstract
The cohesive failure of the adhesive layer of an adhesively-bonded joint behaviour under uniaxial tensile loads in static conditions is analysed by a finite element model as an approximation to the behaviour of adhesively-bonded repairs. A three-dimensional numerical model of a single lap joint was developed using the commercial code Abaqus and validated with results extracted from the literature. The effect of different cohesive law shapes and adhesive properties on the failure load and stresses of the joint was analysed.

1. Introduction

Nowadays, several fields, such as the aircraft industry, use composite materials due to its excellent mechanical and lightness properties. In that industry, this fact represents a reduction in the weight and, consequently, lower fuel consumption. Furthermore, the high level of integration and the large size of the components may make difficult its replacement when they are damaged. Thus, repair damaged parts is in an efficient solution.

Adhesively-bonded repairs offer certain advantages in contrast to mechanical repairs, in particular for thin laminates. Most repair techniques involve removing material from the damaged area, creating a hole. This hole modify the state of load on the structure due to the appearance of stress concentrations around. Adhesively patch repairs are designed to minimise these stress concentrators without adding weight. However, these repairs present non-uniform shear and peeling stresses distributions inside the adhesive that give stress concentrations in the overlap edges, resulting that the adhesive failure is the main damage mechanism. The overall failure of a repaired plate is sensitive to the damage evolution, and the adhesive properties and parameters related [1-2].

In this work, the behaviour of an adhesively-bonded single-lap joint subjected to uniaxial tensile loads in static conditions was analysed as an approximation to the behaviour of adhesively-bonded repairs. The effect of the variation of cohesive law shape and certain cohesive parameters, such as cohesive strength and fracture toughness, on the failure load and stresses was studied.

Excerpt from ISBN 978-3-00-053387-7

2. Problem description

In order to study the behaviour of a single-lap joint under uniaxial tensile loads, a geometry composed of two laminates of unidirectional carbon-epoxy, $[0]_{16}$ lay-up and a total adherend thickness of 2.4 mm, bonded with an epoxy adhesive, Araldite 2015, was analysed. The total length between the two end edges is 240 mm, while the depth of the joint is 15 mm. The overlap length varied from 10 mm to 80 mm (Fig. 1). The geometry was taken from the literature [3] in order to validate the numerical model developed.

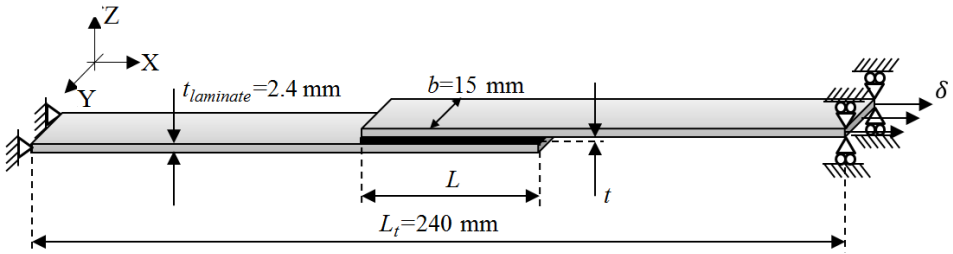

Figure 1. Geometry and boundary conditions of single-lap joint.

This work is focused on the analysis of the cohesive failure of the adhesive layer under tensile loads. Thus, its important to study the influence of different cohesive parameters related to the adhesive properties.

2.1. Numerical model

A 3D numerical model was implemented using the finite element code Abaqus/Standard. The adherends were modelled as orthotropic, linear elastic (Table 1). The adhesive was modelled by using the mixed-mode CZM formulation with a traction-separation law, TSL (Table 2). Experimental test conditions were simulated: one of the edges was clamped, while the opposite end was pulled in tension by imposing a constant and uniform displacement through this end (Fig. 1).

Table 1. Elastic orthotropic properties of the adherends in the fibres direction [3].

Elastic modulus [MPa]	Poisson ratio	Shear modulus [MPa]
$E_x=109\cdot10^3$	$\nu_{xy}=0.342$	$G_{xy}=4315$
$E_y=8819$	$\nu_{xz}=0.342$	$G_{xz}=4315$
$E_z=8819$	$\nu_{yz}=0.380$	$G_{yz}=3200$

Table 2. Adhesive properties of the Araldite 2015 for CZM modelling [3].

Elastic and shear modulus [GPa]	Fracture toughness [N/mm]	Cohesive strength [MPa]
E=1.85 G=0.56	$G_n^C=0.43$	$t_n^0=21.63$
	$G_s^C=4.70$	$t_s^0=17.90$
	$G_t^C=4.70$	$t_t^0=17.90$

The adhesive stiffness was defined as the ratio of the normal modulus (E) and shear modulus (G) to its thickness (t), Eqs. (1) and (2)

Excerpt from ISBN 978-3-00-053387-7

$$K_n = \frac{E}{t} \tag{1}$$

$$K_s = K_t = \frac{G}{t} \tag{2}$$

where K_n, K_s and K_t are the stiffness of the cohesive elements in the normal and shear directions.

A sensitivity analysis of the mesh was carried out to ensure that the results were accurately. Eight-node continuum shell elements with reduced integration (SC8R in Abaqus) were used to mesh of the adherends, while eight-node three-dimensional cohesive elements (COH3D8 in Abaqus), compatible with the previous elements used, were employed to mesh the adhesive layer.

2.2. Progressive damage analysis

The adhesive response was defined by CZM which reproduces the adhesive behaviour in terms of cohesive traction-separation response. Two stages are clearly differenciated: a damage initiation until a stress peak is achieved and a damage evolution that produces a stiffness reduction up to failure due to the progressive adhesive degradation. The initial behaviour is defined by a constitutive elastic matrix that relates the nominal stresses to the nominal strains across the interface (Eq. 3).

$$t = \begin{Bmatrix} t_n \\ t_s \\ t_t \end{Bmatrix} = \begin{bmatrix} K_{nn} & K_{ns} & K_{nt} \\ K_{ns} & K_{ss} & K_{st} \\ K_{nt} & K_{st} & K_{tt} \end{bmatrix} \begin{Bmatrix} \varepsilon_n \\ \varepsilon_s \\ \varepsilon_t \end{Bmatrix} = K\varepsilon \tag{3}$$

where t_n, t_s and t_t are the traction stresses in the normal and shear directions respectively while ε_n, ε_s and ε_t represent the strains in those same directions. Meanwhile, K is the stiffness matrix related to the adhesive properties.

The beginning of the degradation of the material is determined by the chosen damage initiation criterion. Between the criteria available in Abaqus, a quadratic nominal stress criterion has been chosen in this work (Eq. 4)

$$\left\{\frac{\langle t_n \rangle}{t_n^0}\right\}^2 + \left\{\frac{t_s}{t_s^0}\right\}^2 + \left\{\frac{t_t}{t_t^0}\right\}^2 = 1 \tag{4}$$

The material damage occurs according to a damage evolution law (Eq. 5), which describes adhesive stiffness degradation rate. Thus, a scalar damage variable D, that represents the overall damage in the adhesive, is defined. When the adhesive is undamaged, that is, a behaviour corresponding to the elastic region, D has a value of 0. After the initiation of the damage this value increases until 1, when the material is fully damaged.

$$\begin{aligned} t_n &= \begin{cases} (1-D)\bar{t}_n \longrightarrow \bar{t}_n \geq 0 \\ \bar{t}_n \longrightarrow \text{No damage} \end{cases} \\ t_s &= (1-D)\bar{t}_s \\ t_t &= (1-D)\bar{t}_t \end{aligned} \tag{5}$$

where $\bar{t}_n$, $\bar{t}_s$ and $\bar{t}_t$ are the traction stresses in each direction predicted by the elastic traction-separation behaviour without damage.

Excerpt from ISBN 978-3-00-053387-7

Different shapes of damage evolution can be used. In this work, the influence of linear, exponential and trapezoidal damage evolution laws was analysed (Fig. 2).

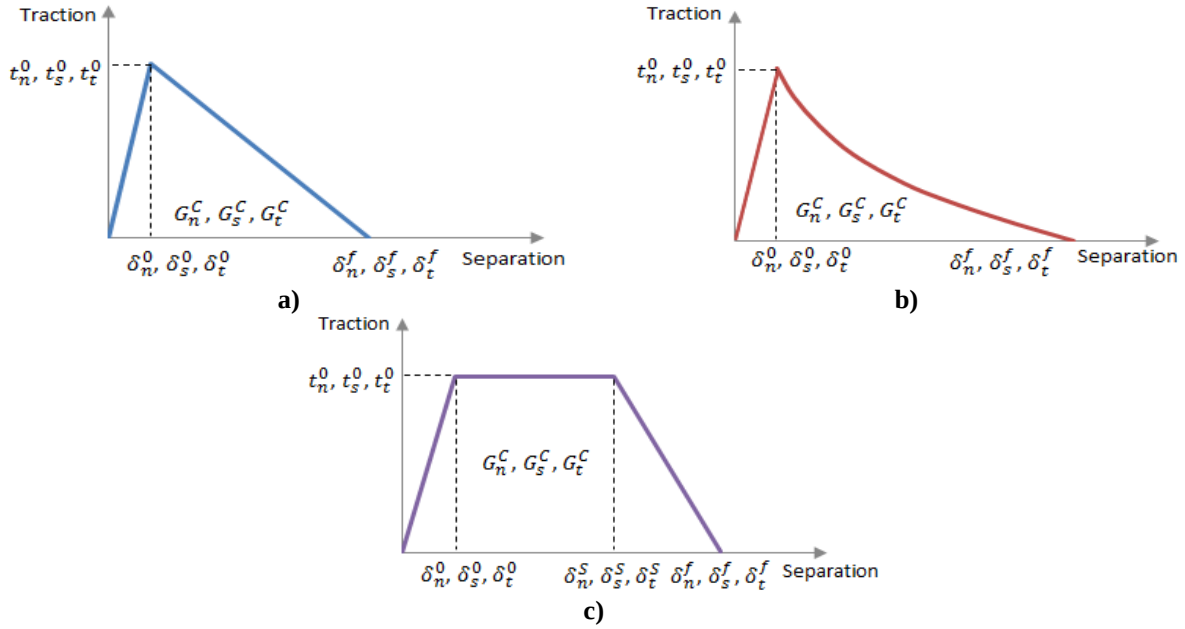

Figure 2. Damage evolution laws analysed: a) linear law, b) exponential law and c) trapezoidal law.

2.3. Model validation

The 3D numerical model results obtained were validated comparing with the 2D numerical and experimental data available in the literature [3]. The variable used in the validation was the load-displacement curve. The linear damage evolution law (Fig. 2a) was considered in both numerical models.

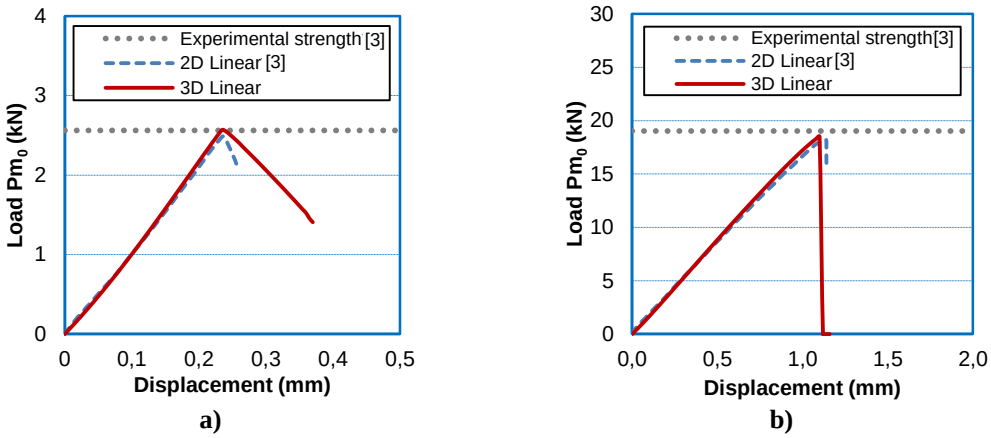

Figure 3. Load-displament validation curves for overlp lengths of a) L_0=10 mm and b) L_0=80 mm.

The numerical results obtained from the 3D model developed are in great agreement with both experimental and 2D numerical results taken from the literature. The maximum load value for 10 mm overlap length is 2.57 kN, while for 80 mm is 18.50 kN. The differences between them and results from the literature are less than 5% in either case.

Excerpt from ISBN 978-3-00-053387-7

3. Results

3.1. Effect of the cohesive law shape

The numerical failure load for overlap lengths ranging between 10 mm and 80 mm using linear, exponential and trapezoidal cohesive laws was studied. Fig. 4 shows the results in percentage variations of the maximum load attained between the 3D numerical model results and the experimental data taken from the literature [3], which were in great agreement showing variations less than ±7% for any cohesive law considered.

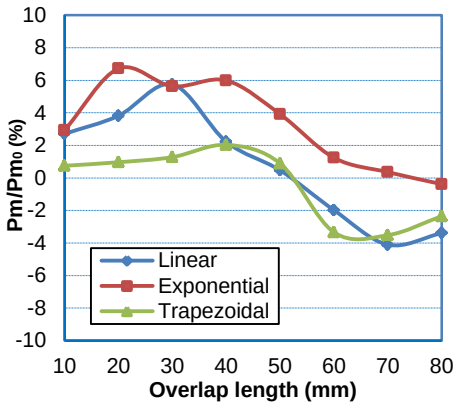

Figure 4. Numerical results compared with experimental results [3] for the different TSL.

Both linear and trapezoidal laws overestimated the failure load for overlaps below 40 mm; however, for overlaps above 40 mm, this value was underestimated. The exponential law overestimated the failure load for the full range of lengths analysed. In view of the results, the trapezoidal law presented the best fit to the experimental results; therefore from this point on, the trapezoidal law is considered.

3.2. Stress analysis

The effect of the variation of the overlap length on normal and shear stress along the adhesive mid-thickness was analysed. Both stresses were normalized by τ_{avg} (the average value of τ_{xz}) and the position along the adhesive thickness by the overlap length L_0 (Fig. 5).

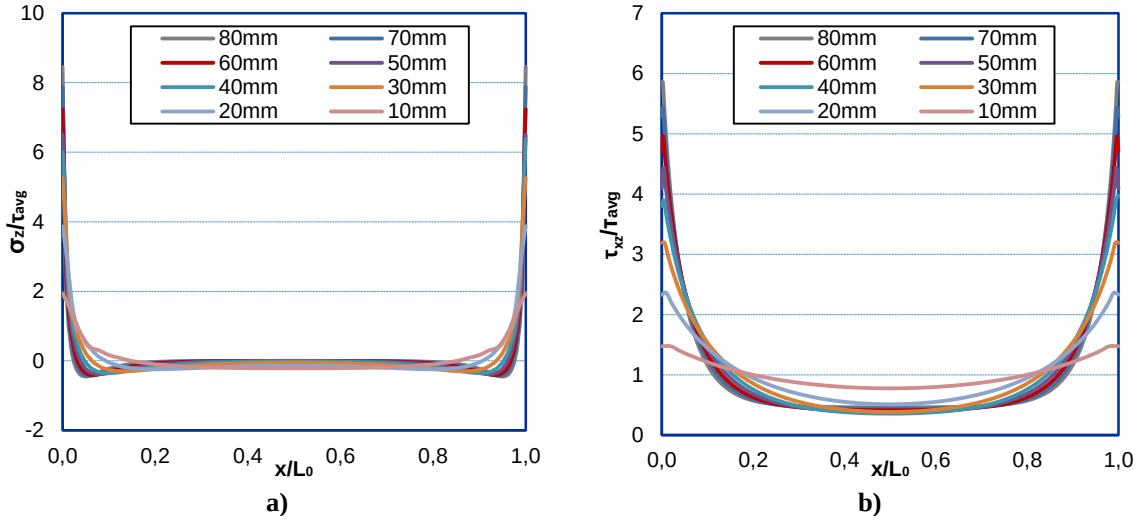

Figure 5. Stress profiles for different overlap lengths: a) normal stress and b) shear stress.

Excerpt from ISBN 978-3-00-053387-7

Peel stresses present singularities at the edges of the bonded area which result in large stress gradients near them. The increment of the overlap length produces an increase of the maximum peel stress values (Fig.6).

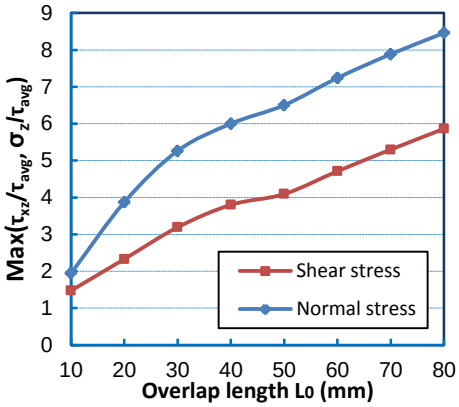

Figure 6. Variation of the maximum values of normal and shear stresses with the overlap length.

Additionally, stress concentrations, which appear due to the eccentricity of load resulting in the bending of adherents and its separation, increase with the increment of the overlap length. In the middle of the bonded area the stresess values are negative, so compressive stresses appear (Fig. 7).

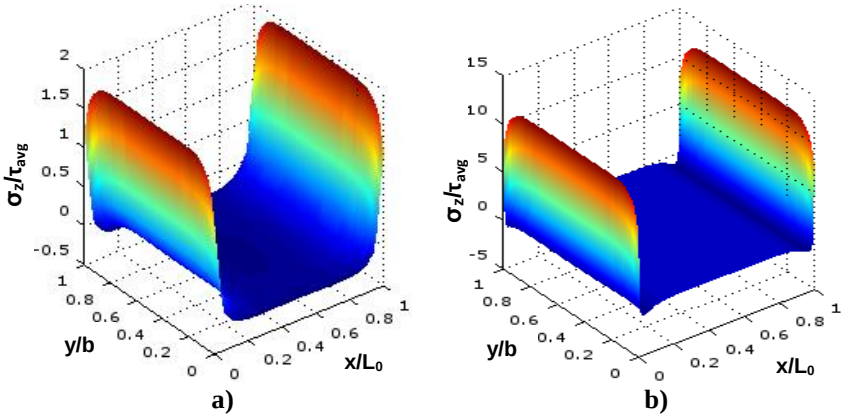

Figure 7. 3D peel stress profiles for different overlap length: a) 10 mm and b) 80 mm.

Shear stresses have a concave shape due to the progressive distribution of stresses produced within the adhesive. The concavity increases as the overlap length increments its value (Fig. 8). The increment of the overlap length leads to an increase of the maximum peel stress values (Fig. 6).

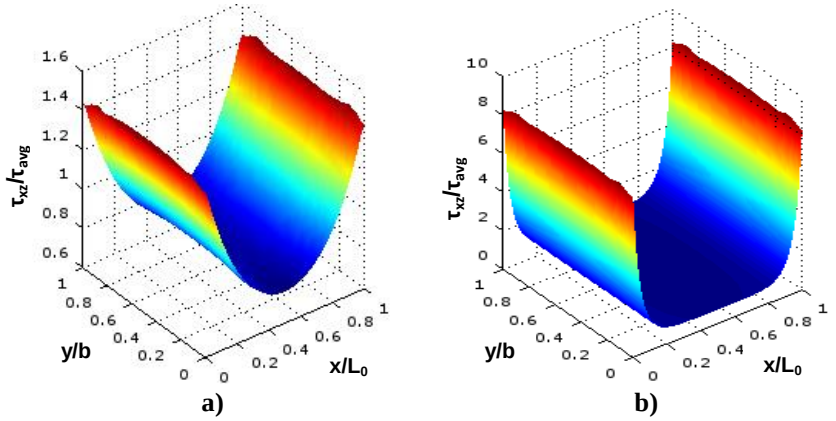

Figure 8. 3D shear stress profiles for different overlap length: a) 10 mm and b) 80 mm.

Excerpt from ISBN 978-3-00-053387-7

3.3. Effect of the variation of cohesive parameters

The influence of the damage evolution law on the failure load of the joint, fracture toughness and cohesive strength was studied for different overlap lengths (10 mm, 30 mm, 60 mm and 80 mm). Both cohesive paramenters were varied by -50%, +50% and +100% separately (Fig. 9). These changes are applicable on both normal and shear directions.

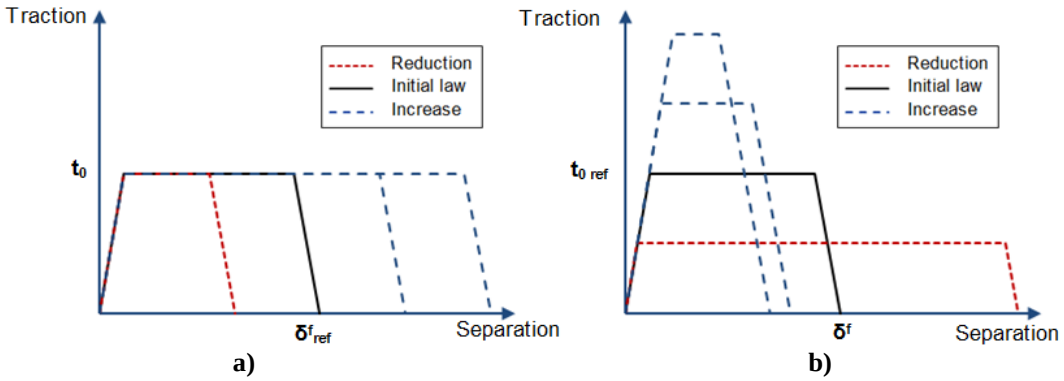

Figure 9. Trapezoidal cohesive law: variation of the a) adhesive toughness and b) cohesive strength.

The results are presented in percentage variations (Fig. 10), as the ratio of the maximum load attained for the modified cohesive parameter (Pm) to the maximum load for the reference case with the original cohesive parameters (Pm_0). An increase the fracture toughness, produces variations on the maximum load smaller than +2% (Fig. 10a). When decreasing the cohesive parameter by -50%, only the longest overlap presented a more significant variation (-15.38%), due to the increase of the maximum shear stress, resulting in the reduction of the maximum load.

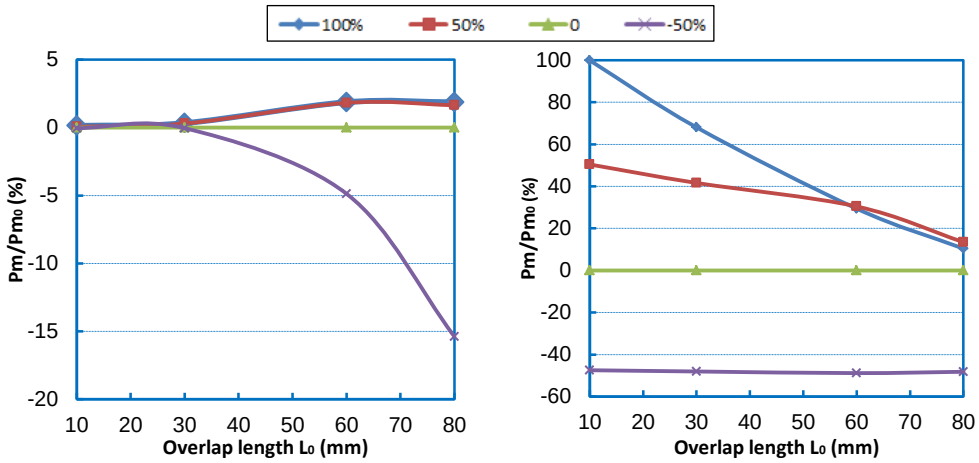

Figure 10. Effects of the variation of the cohesive parameters of the trapezoidal law varying a) the fracture toughness and b) the cohesive strength.

For the overlap lengths studied, the failure load were reduced a -48% approximately when decreasing the cohesive strength (Fig. 10b). When increasing this parameter, significant variations occurred for L_0=10 mm and L_0=30 mm. However, for L_0=60 mm and L_0=80 mm the increment of the cohesive strength by +100%, produces a decrement in the maximum load, about 1% and 3% respectively, regarding to results with cohesive strength by +50%. This is due to the similarity between the modified trapezoidal law and an equivalent linear law with the same cohesive strength and final relative displacement.

Excerpt from ISBN 978-3-00-053387-7

4. Conclusions

In this work, the influence of the damage evolution law and the variation of cohesive parameters on the behaviour of an adhesively single-lap joint under uniaxial tensile loads in static conditions was studied. Virtual tensile tests were performed by developing a numerical model using Abaqus/Standard validated with available results in the literature.

Maximum load values of the 3D numerical model were higher than the obtained in the 2D numerical model from the literature [3], and therefore more conservative. The cohesive laws studied showed differences below the ±7% in any case between numerical and experimental results. The trapezoidal law presented closer results to the experimental ones, since the adhesive considered is a ductile adhesive that showed a large plastic flow, and this behavior was captured.

Thereby, the use of the suitable cohesive law shape is important according to the adhesive employed and its behaviour. For longest overlap lenghts (L_0=60 mm and L_0=80 mm) and higher variations of the cohesive strength (+100%), the trapezoidal law presented variations below the maximum reference load due to the similarity of the modified law to an equivalent linear law. Thus, for overlap lengths above 40 mm, the variation of the cohesive strength does not describe the plastic flow inside the adhesive, since the second part of the curve (where the stresses are constant) is shorter than the reference law.

Acknowledgments

The authors are indebted for the financial support of this work to the Ministry of Economy and Competitiveness of Spain (project DPI2013-42240-R).

References

[1] G.Alfano. On the influence of the shape of the interface law on the application of cohesive-zone models. *Composites Science Technology*. 66:723-730 (2006).

[2] M.Ridha, V.B.C.Tan, T.E.Tay. Traction-separation laws for progressive failure of bonded scarf repair of composite panel. *Composite Structures*. 93:1239-1245 (2011).

[3] R.D.S.G.Campilho, M.D.Banea, J.A.B.P.Neto, L.F.M.da Silva. Modelling adhesive joints with cohesive zone models: effect of the cohesive law shape of the adhesive layer. *International Journal of Adhesive and Adhesion*. 44:48-56 (2013).

Excerpt from ISBN 978-3-00-053387-7